

General Disclaimer

One or more of the Following Statements may affect this Document

- This document has been reproduced from the best copy furnished by the organizational source. It is being released in the interest of making available as much information as possible.
- This document may contain data, which exceeds the sheet parameters. It was furnished in this condition by the organizational source and is the best copy available.
- This document may contain tone-on-tone or color graphs, charts and/or pictures, which have been reproduced in black and white.
- This document is paginated as submitted by the original source.
- Portions of this document are not fully legible due to the historical nature of some of the material. However, it is the best reproduction available from the original submission.

X-621-69-42

PREPRINT

NASA TM X-63496

**A THEORY OF THERMOSPHERIC
DYNAMICS·PART II GEOMAGNETIC
ACTIVITY EFFECT, 27 DAY VARIATION
AND SEMIANNUAL VARIATION**

H. VOLLAND

FEBRUARY 1969



**— GODDARD SPACE FLIGHT CENTER —
GREENBELT, MARYLAND**

FACILITY FORM 602

<u>N 69-21409</u>	
(ACCESSION NUMBER)	(THRU)
<u>35</u>	<u>1</u>
(PAGES)	(CODE)
<u>TMX-63496</u>	<u>13</u>
(NASA CR OR TMX OR AD NUMBER)	(CATEGORY)

X-621-69-42

A THEORY OF THERMOSPHERIC DYNAMICS
PART II
GEOMAGNETIC ACTIVITY EFFECT,
27 DAY VARIATION AND SEMIANNUAL VARIATION

by

H. Volland*

February 1969

*NAS/NRC research associate on leave from the Astronomical Institutes of the
University of Bonn, Germany.

GODDARD SPACE FLIGHT CENTER
Greenbelt, Maryland

PRECEDING PAGE BLANK NOT FILMED.

A THEORY OF THERMOSPHERIC DYNAMICS

PART II

GEOMAGNETIC ACTIVITY EFFECT,

27 DAY VARIATION AND SEMIANNUAL VARIATION

H. Volland

Goddard Space Flight Center

Greenbelt, Maryland

ABSTRACT

The geomagnetic activity effect, the 27 day variation and the semiannual variation of the thermospheric density are nearly independent of local time. Therefore, they are treated by a one dimensional model in order to find out the height distribution and the amount of energy necessary to create the observed amplitudes and phases of the neutral density between 120 and 400 km altitude. Three types of heat energy sources have been considered which simulate energy input: I at the bottom of the thermosphere; II within the thermosphere; and III at the top of the thermosphere. The geomagnetic activity effect and the 27 day variation can be described as generated by heat source II which is interpreted as resulting from corpuscular radiation into the aurora zones and from solar active region EUV radiation, respectively. The semiannual effect can be described by heat source I and is interpreted as resulting from dissipated energy of a tidal wave from the lower atmosphere. The leakage of the energy of this tidal wave into the thermosphere shows a semiannual variation which creates the observed density variations. Quantitative calculations give the amount of energy of the various heat sources, amplitudes and phases of the generated density and temperature variations and their dependence on solar activity.

A THEORY OF THERMOSPHERIC DYNAMICS

PART II

GEOMAGNETIC ACTIVITY EFFECT,

27 DAY VARIATION AND SEMIANNUAL VARIATION

1. INTRODUCTION

In part I of this paper (Volland, 1968) (referred to as paper I) we used a two dimensional model of the thermosphere, valid at low latitudes, to reproduce the diurnal variation and the solar cycle variation of the thermospheric density between 100 and 400 km altitude. This model requires that besides the solar EUV radiation, which had been assumed to be proportional to the 10.7-cm solar flux \bar{F} , a tidal wave of constant amplitude penetrates from the lower atmosphere into the thermosphere. The tidal wave dominates the density variations below 250 km height and is significant even at 400 km height.

In this paper we shall deal with the geomagnetic activity effect, with the 27 day variation and with the semiannual variation of the thermospheric density. All three effects are nearly independent of local time which means that the energy input into the thermosphere occurs on a global scale. Therefore, we can treat these effects theoretically by a one dimensional model in which horizontal exchange of mass, momentum and energy is neglected. We shall consider three different heat sources as generators of the density disturbances which represent energy input into the entire thermosphere, at the bottom and at the top of the thermosphere. The two last heat sources shall simulate a wave input from below and from above respectively into the thermosphere. We shall compare the

theoretically results with available density observations and shall select the respective heat sources which optimally describe the measured density variations of the different effects in amplitude and phase and their dependence on height and solar cycle.

2. THE MODEL

Our two dimensional model is based on perturbation theory which is a sufficient approximation for thermospheric diurnal tides below 400 km altitude. Perturbation theory results in a decoupling of the disturbances due to the different energy sources. In the case of the diurnal tide we therefore could separate by a mathematical method the density and temperature variations which were generated by an internal EUV heat source within the thermosphere on the one hand and those which were due to a tidal wave from the lower atmosphere on the other hand. The energy sources and the physical parameters of the thermospheric diurnal tide can be written in general form as

$$c(y, z, t) = c_0(z, t) + \Delta c_{\text{diurn}}(z, t) \cos\{\Omega(\tau - \tau_{\text{diurn}}(z))\} \quad (1)$$

where

$$\Delta c_{\text{diurn}} \cos\{\Omega(\tau - \tau_{\text{diurn}})\} = \Delta c_{\text{EUV}} \cos\{\Omega(\tau - \tau_{\text{EUV}})\} + \Delta c_{\text{tide}} \cos\{\Omega(\tau - \tau_{\text{tide}})\}$$

is the diurnal component consisting of an EUV component and a tidal component and c_0 is the mean component averaged over one solar day. τ_{diurn} , τ_{EUV} and τ_{tide} are the times of maximum of the different components, y is the

longitudinal coordinate along the equator, z is the height, t the universal time, $\tau = t + \frac{y}{R\Omega}$ the local time, R the Earth's radius and Ω the angular frequency of the earth's rotation. c_0 and Δc_{diurn} are height dependent. For the 27 day variation and the semiannual effect they are also slowly varying with time with periods large compared with one solar day. However, during a geomagnetic activity effect the time variation of c_0 occurs with a quasiperiod which is of the order of one solar day. We write

$$\begin{aligned} c_0(z, t) &= \overline{c_0(z)} + \Delta c_0(z) \cos \{ \omega (t - t_0(z)) \} \\ \Delta c_{\text{diurn}}(z, t) &= \overline{\Delta c_{\text{diurn}}(z)} + \Delta \Delta c_{\text{diurn}}(z) \cos \{ \omega (t - t_{\text{diurn}}(z)) \} . \end{aligned} \quad (2)$$

ω is the angular frequency of one of the disturbances which we will consider in this paper: geomagnetic activity effect, 27-day variation or semiannual effect. Δc_0 and $\Delta \Delta c_{\text{diurn}}$ are the amplitudes of those disturbances. $\overline{c_0}$ and $\overline{\Delta c_{\text{diurn}}}$ are mean values averaged over the time of the respective disturbances.

Consistent with the use of perturbation theory we consider the amplitude $\Delta \Delta c_{\text{diurn}}$ of the diurnal disturbance as a second order effect which we shall neglect in the following calculations. This is justified by the observations. E.g., for the 27 day solar rotation effect one derives a maximum temperature increase at day and at night, respectively, of

$$T_D = 2.4(F - \overline{F}) \quad (3)$$

$$T_N = 1.8(F - \overline{F})$$

(Priester et al., 1967; Jacchia, 1964). F is the instantaneous 10.7 cm solar flux (in units of 10^{-22} W/m² Hz) and \bar{F} is a mean value averaged over several solar rotations. Using Equation (3) we determine

$$\Delta T_0 = 2.1(F - \bar{F})$$

$$\Delta\Delta T_{\text{diurn}} = 0.3(F - \bar{F})$$

Thus

$$\frac{\Delta\Delta T_{\text{diurn}}}{\Delta T_0} = \frac{1}{7} \ll 1.$$

Similar estimates can be made for the semiannual effect and for the geomagnetic activity effect. Therefore we shall deal in this paper exclusively with the time variations of the mean values c_0 .

Since the energy inputs into the thermosphere which create the disturbances Δc_0 are world wide and do not depend on local time, the model to treat these disturbances at low latitudes becomes a one dimensional vertical model. The mathematical treatment of this one dimensional model is exactly the same as for the two dimensional model (see paper I). We only have to take the horizontal wavenumber equal to zero, which means neglect of horizontal energy, mass and momentum exchange.

3. THE HEAT SOURCES

One of the problems of thermospheric dynamics is the height distribution and the amount of heat which causes the different density disturbances. This

question is closely related with the generation mechanism of the disturbances. There are essentially three possible ways of energy input into the neutral thermosphere:

- I. Heating at the bottom of the thermosphere by Joule heating or by energy dissipation of a tidal wave from below.
- II. Direct energy input into the thermosphere by solar EUV radiation converted into heat of the neutral air.
- III. Heating at the top of the thermosphere through energy impact of hydro-magnetic waves from the magnetosphere.

All three heating mechanisms have been discussed in the literature as the possible causes for the three different thermospheric disturbances. We shall refer to these references in the following sections. In order to differentiate between the possible energy mechanisms we adopted in this paper three heat energy sources of amplitude Δq_0 varying in time with frequency ω and placed at different heights within the thermosphere. Heat source I (curve I in Figure 1) provides a heat input of constant amplitude between $z_1 = 100$ and $z_2 = 120$ km altitude. Heat source II situated between $z_1 = 120$ and $z_2 = 400$ km altitude has the same height distribution as the EUV heat source in paper I [Equation (8)]. Heat source II is shown in Figure 1 where its amplitude Δq_0 is labelled as curve II. The amplitude of heat source III (curve III in Figure 1) is constant between $z_1 = 400$ and $z_2 = 420$ km and zero elsewhere. Heat sources I and III shall simulate energy inputs into the thermosphere from below and from above. The total heat input of each source

$$\Delta E_0 = \int_{z_1}^{z_2} \Delta q_0(\xi) d\xi \quad (4)$$

will be chosen such that it provides equal density amplitudes at 400 km altitude for all three sources. Because of our linearized problem density and temperature amplitudes are directly proportional to the heat input values.

4. THE GEOMAGNETIC ACTIVITY EFFECT

During geomagnetic disturbances the thermospheric density increases between 160 and 1000 km altitude (Jacchia, 1959). The amplitude of the density disturbance increases with height below the Helium belt. According to Jacchia and Slowey (1964a, 1964b) the intensity of the geomagnetic activity effect, represented by Jacchia's exospheric temperature, is proportional to the planetary geomagnetic index a_p for large disturbances and is proportional to the index K_p for small disturbances. The effect occurs world wide. But the density disturbance appears to be systematically larger and to occur earlier within polar regions than within lower latitudes. The time of the density maximum is delayed by about 5 to 7 hours with respect to the time of maximum of the geomagnetic index a_p (Roemer, 1967a; Jacchia et al., 1966). The time of density maximum seems to be independent on height. The density disturbance has an impulse form with a typical duration of one day.

From these observational facts mentioned above Jacchia (1959) concluded that geomagnetic disturbances and the geomagnetic activity effect have a common cause namely the amplification of the solar wind. There remains the question in what manner the energy of the solar wind is transferred into heat of the thermosphere. Two hypotheses exist to explain this phenomenon:

- a. High energy particles precipitate into the aurora zones and heat directly the neutral thermosphere there. Moreover the increase of the electron density within the aurora zones gives rise to an increase of the electric currents within the ionospheric auroral electro jet. Thus the thermosphere at high latitudes becomes additionally heated by Joule heating. This heating process occurs predominantly between 100 and 200 km altitude (Jacchia, 1966; Cole, 1966) and is transported by heat conduction and heat convection into lower latitudes.
- b. The direct impact of the solar wind on the magnetosphere creates hydrodynamic waves which travel into the upper atmosphere. The dissipation of their energy or the coupling between hydromagnetic waves and heat conduction waves causes a heating of the thermosphere from above (Dessler, 1958; Volland, 1967).

In order to test these hypotheses we apply a one dimensional vertical model in which a harmonic wave with the period of $\Delta\tau = 1.15$ days (angular frequency: $\omega = 2\pi/\Delta\tau = 6.3 \times 10^{-5} \text{ sec}^{-1}$, equivalent to the predominant frequency within a typical impulse type disturbance) generates neutral air waves. This model is of course a gross simplification. In an exact treatment of the geomagnetic activity effect one has to consider the entire frequency spectrum of the impulse. Nevertheless, we shall see that essential features of the observations can be interpreted by such simple model.

We suppose that the maximum heating of the thermosphere coincides with the maximum of the geomagnetic disturbance. The specific impulse time of

$\Delta\tau = 1.15$ days had been chosen in our model such that the observed time lag in the density can best be reproduced. Since the observed duration of geomagnetic activity effects varies between about 0.5 and 2 days this impulse time is a reasonable average value.

The response of the neutral thermosphere to the three different heat sources of angular frequency ω and with amplitudes Δq_0 according to Figure 1 has been calculated. The density and temperature variations resulting from these three heat generators are plotted versus height in Figure 2 (relative amplitude) and Figure 3 (time lag between maximum heating and maximum density and temperature variations). The basic thermospheric model adopted in those calculations was the Jacchia model at $\bar{T}_\infty = 1000^\circ\text{K}$ (for details see paper I).

For comparison the dashed lines in Figure 2 give the relative density and temperature amplitudes determined from the Jacchia-model (Jacchia, 1964) at $\bar{T}_\infty = 1000^\circ\text{K}$ ($\bar{F} = 125$) and for an exospheric temperature amplitude of $\Delta T_\infty = 100^\circ\text{K}$. According to Jacchia et al. (1966) the height distribution of the density amplitude of the geomagnetic activity effect is similar to that of the diurnal variation represented by the dashed line in Figure 2a.

Figure 4 gives the absolute amplitudes of density and temperature at 400 km altitude versus solar activity factor \bar{F} calculated with the same heat input of heat source II. It shows that the density amplitude increases and the temperature amplitude decreases with \bar{F} , which results merely from the changing propagation conditions for the waves within the thermosphere.

From Figures 2 and 3 we can immediately exclude heat sources I and III as the sole causes for the geomagnetic activity effect, because the height dependence of the density amplitude in model I and the height dependence of the time lag in model III are inconsistent with the observations. The last point has been predicted already by Thomas and Ching (1968) from a more sophisticated model.

Heat input II can explain rather well the observed height distribution of the density variation as well as the time lag of about 6 hours between maximum heating and maximum density. [See the dashed lines in Figures 2a and 3a which give the relative density amplitude of the Jacchia model and the density time lag determined by Roemer (1967a) and Jacchia et al. (1966).]

The time lag $(t_0)_{\text{geomagn}}$ of each individual effect of course depends on its respective impulse duration $\Delta\tau$ (in days) and is for heat source II approximately

$$(t_0)_{\text{geomagn}} \sim 0.18 \Delta\tau$$

at 400 km altitude.

From these calculations we have to exclude hypothesis (b) — the direct heat input from the magnetosphere into the thermosphere — as the origin of the geomagnetic activity effect. Hypothesis (a) — aurora zone heating and subsequent heat transport into the lower latitudes — then describes most likely the energy input distribution of that effect.

A nearly complete agreement between observations and theory could be achieved from a combination between heat sources I and II with energy inputs of both sources which are of the same order of magnitude. This is equivalent to a

heat distribution with a scale height increasing with altitude. In view of the very crude approximations made in this model we did not pursue this point further. From the same argument we should consider the following numerical data merely as estimates.

According to the observations a geomagnetic index of $K_p = 5$ is related to an exospheric temperature increase of the Jacchia model of

$$\Delta T_{\infty} = 100^{\circ}\text{K}$$

which corresponds at 400 km altitude to a relative density amplitude of

$$\frac{\Delta \rho_0}{\rho_0} = 0.39 \text{ for } \bar{F} = 125.$$

According to Figure 2 such density amplitude is generated by heat source II with a total heat input of

$$(\Delta E_0)_{\text{geomagn}} = 0.31 \text{ erg/cm}^2\text{sec}. \quad (5)$$

The temperature amplitude created by heat source II is $\Delta T = 120^{\circ}\text{K}$ (see Figure 2b). The larger temperature amplitude in our model compared with Jacchia's exospheric temperature increase results from the different density and temperature versus altitude profiles adopted in both models. Since we neglect in our model the diurnal variation of the molecular weight (see paper I) the temperature difference between our and Jacchia's data is underestimated and becomes even larger if we take into account the temporal variation of the molecular weight.

Roemer gave an empirical formula of Jacchia's exospheric temperature increase as function of the K_p index [see Equation (2.5) in Priester et al., 1967]. Using the result of our Equation (5) we can transform that formula into a relationship between K_p and heat input:

$$(\Delta E_0)_{\text{geomagn}} = 3.1 \times 10^{-3} \left(20 K_p + 0.03 e^{K_p} \right) \text{ erg/cm}^2\text{sec} . \quad (6)$$

According to Equation (6) during very strong geomagnetic storms ($K_p \gtrsim 8$) a total heat input of $(\Delta E_0)_{\text{geomagn}} \gtrsim 1 \text{ erg/cm}^2\text{sec}$ into the thermosphere is necessary to increase the density to the observed value. If that heat input is provided exclusively from the aurora zones, a heat input of the order of $\gtrsim 100 \text{ erg/cm}^2\text{sec}$ has to be provided into the aurora belts. According to O'Brien and Taylor (1964) the energy flux of high energy particles can increase up to $2000 \text{ erg/cm}^2\text{sec}$ during severe geomagnetic storms. Taking an efficiency factor of 0.1 for the transformation of particle energy into heat energy of the neutral air, we come up with the right order of magnitude to explain the geomagnetic activity effect by aurora heating of high energetic particles.

The energy transport from the aurora zones into the lower latitudes remains a problem. Joule heating at ionospheric heights within low latitudes must be ruled out because the electric currents during geomagnetic storms flow outside the ionosphere (Langel and Cain, 1968; Cain, personal communication). Probably it is mainly heat convection and heat conduction by which the "line sources" within the aurora zones distribute their energy into the entire thermosphere.

5. 27 DAY-SOLAR ROTATION EFFECT

On the surface of the sun certain long-lived activity regions with excessive EUV radiation can exist near coronal condensations. These regions rotate with the sun with a period of 27 days. Their varying energy input into the thermosphere can be observed as thermospheric density variations with periods of 27 days (Jacchia and Briggs, 1958; Priester, 1959). The relationship between solar activity number F and the exospheric temperature of the Jacchia model (Jacchia, 1964) is given by Equation (3). The time delay between the maximum of the density variation and the maximum of the correspondent excessive EUV radiation is 2.3 days according to MacDonald (1963) and one day above 350 km according to Roemer (1967b). The height dependence of the density variations is similar to that of the geomagnetic activity effect (see section 4). Blum (1969) has shown that an appropriate energy input from the exosphere into the thermosphere can shift the time delay of the density maximum to the desired value.

Our model to describe this effect consists again of a one dimensional vertical model in which a heat source with a height distribution equal to the EUV heat source (source II in Figure 1) and with a period of $\Delta\tau = 27$ days (angular frequency $\omega = 2.7 \times 10^{-6} \text{ sec}^{-1}$) generates waves within the neutral thermosphere. The results of these calculations are shown in Figure 5 (relative amplitude) and Figure 6 (time delay between maximum heating and maximum density and temperature variation), where density and temperature variations are plotted versus height. The basic thermospheric model is again the Jacchia model at $\bar{F} = 125$.

Jacchia (1964) observed that the height distribution of the amplitude of the 27 day variation is similar to the height profile of the diurnal variation. In Figure 5 the dashed lines give the relative density and temperature amplitudes of the Jacchia model (Jacchia, 1964) for $\bar{F} = 125$. We notice sufficient agreement in their height dependence between the density distribution of heat source II (curve II) and the data of the Jacchia model above 200 km altitude. From Figure 6 we observe that the natural time response of the thermospheric density with respect to heat source II is 2 days at 400 km altitude which lies between the numbers observed by Roemer (1967b) and McDonald (1963) (see the dashed lines in Figure 6b).

For comparison we also plotted in Figures 5 and 6 the 27 day variations of density and temperature due to heat sources I and III. Heat source I can be excluded as the origin of the 27 day variation because the time delay of 6 days as well as the height dependence of the density variation are inconsistent with the observations. Heat sources II and III generate similar density variations. However in order to generate the same density amplitude at 400 km height the temperature amplitude of source III is nearly twice as large as the temperature amplitude of heat source II while the total energy input of heat source III is only half the input of source II. Therefore only a temperature measurement can decide whether a heat input of the general form of source II or of source III is responsible for the 27 day variation, though heat source II approximates most likely the real energy source considering its generation mechanism.

The total heat input of heat source II in Figure 5 has been chosen such that it creates a density variation equivalent to an increase of the exospheric temperature in the Jacchia model of

$$\Delta T_{\infty} = 100^{\circ}\text{K at } \bar{F} = 125 .$$

From Figure 5 and from Equation (3) we derive a relationship between excessive EUV heat input and solar activity factor F :

$$(\Delta E_0)_{27d} = 1.19 \times 10^{-3} (F - \bar{F}) \text{ erg/cm}^2\text{sec for } \bar{F} = 125 . \quad (7)$$

The temperature variation due to heat source II in our model is smaller than that of the Jacchia model:

$$\frac{\Delta T_0}{\Delta T_{\infty}} = 0.70 \text{ at 400 km altitude.}$$

This difference results from our neglect of a time varying molecular weight (for details see paper I).

Figure 7 gives the absolute amplitudes of density and temperature of heat source II versus solar activity factor \bar{F} . The density amplitude increases by a factor of 4 between minimum and maximum conditions though the excessive EUV heat input remains the same. However the relative density amplitude decreases with increasing \bar{F} because ρ_0 increases stronger than $\Delta\rho_0$. These features are consistent with the observations (Jacchia, 1966).

6. SEMIANNUAL EFFECT

The semiannual variation of the thermospheric density with its maximum during April and October has been discovered by Pätzold and Zschörner (1960). This effect can be observed between 150 and 1500 km altitude in the density

(King-Hele, 1968; Cook and Scott, 1966). The relative density amplitude only slightly increases with height. At 190 km altitude King-Hele (1968) observed a ratio between maximum and minimum density of $f = 1.45$. The density amplitude increases with solar activity and is proportional to \bar{F} (Jacchia et al., 1968).

A semiannual effect can likewise be observed in the geomagnetic S_q variations (e.g. Wagner, 1968), in the geomagnetic activity (e.g. Priester and Cattani, 1962), in the virtual height of the F2 maximum (Becker, 1966), in the electron density of the F2 peak (Yonezawa, 1967), in the electric and neutral components of the mesosphere (e.g. Lauter et al., 1966) and in the wind circulation within mesosphere (Kochanski, 1964) and stratosphere (Quiroz and Miller, 1967; Newell, personal communication).

Several hypotheses try to explain this effect either by the solar wind impinging on the magnetosphere (Pätzold and Zschörner, 1960; Priester and Cattani, 1962), by a semiannual variation of the height of the turbopause (Cook, 1966) or by a change in the mesospheric circulation system of the wind [Johnson, (see Jacchia, 1965); Newell, 1968]. A review article about the semiannual effect is given by Harris and Priester (1969).

Our explanation of the semiannual effect follows closely an idea of Newell (1968): A semiannual oscillation of the stratospheric wind is related to the semiannual change of the polar vortex from the summer into the winter hemisphere during the equinox. The generation and the propagation characteristics of the diurnal tidal wave within the lower atmosphere are influenced by those winds. The diurnal component of the tidal wave within the lower atmosphere is

of an evanescent wave type. Therefore changing prevailing wind systems might be responsible for a variation in the leakage of wave energy flux of the tidal wave into the upper atmosphere. Thus the amplitude of the tidal wave is modulated with a semiannual period, which causes the various mesospheric semiannual effects. Within E-layer heights the horizontal wind of the tidal wave, which generates the S_q variations, creates a semiannual variation of the S_q current. Since the S_q current is proportional to the electron density, we expect an increase of the semiannual amplitude of the S_q current with increasing solar activity. This has been in fact observed (Wagner, 1968).

In paper I we estimated a time averaged wave energy input of the tidal wave at 100 km altitude of $0.1 \text{ erg/cm}^2 \text{ sec}$. This energy is totally dissipated within the thermosphere and contributes to the mean thermospheric heat input in addition to the EUV heat input. It is our hypothesis that the semiannual variation of this tidal wave dissipation generates the semiannual variation of the thermospheric density. That heating has a component averaged over one day and a diurnal component [ΔE_0 and $\Delta \Delta E_{\text{diurn}}$ in Equation (2)]. Because of our use of perturbation theory we only can deal with the averaged component $(\Delta E_0)_{\text{semi}}$ though one observes from the behavior of the S_q current that the diurnal component $(\Delta \Delta E_{\text{diurn}})_{\text{semi}}$ is of significant influence at least within the lower thermosphere.

In order to test our hypothesis we repeated the calculations performed in sections 4 and 5 taking now a period of $\Delta \tau = 182.5 \text{ days}$ equivalent to an angular frequency of $\omega = 4 \times 10^{-7} \text{ sec}^{-1}$. To adjust our theoretical density values to the observed data we derived from Jacchia's observations (Jacchia et al., 1968)

a relative density amplitude of the semiannual effect at 400 km altitude of

$$\frac{\Delta \rho_0}{\rho_0} = 0.24 \text{ for } \bar{F} = 125 (\bar{T}_\infty = 1000^\circ\text{K})$$

corresponding to an increase of Jacchia's exospheric temperature of

$$\Delta T_\infty = 60^\circ\text{K}.$$

Figures 8 and 9 show the relative amplitudes of the density and temperature variations and the time delay between maximum heat input and maximum density and temperature plotted versus height. These were calculated for the three heat sources I, II and III. The Jacchia model at $\bar{F} = 125$ was used. From these figures we can exclude heat sources II and III as the cause of the semiannual effect because the resulting density disturbances do not penetrate deep enough into the lower thermosphere to generate the various effects observed there. Heat source I describes well the observations, namely the slight increase of the relative density amplitude with height and the rather large density amplitude at 190 km altitude observed by King-Hele (1968). Note that between 140 and 400 km the relative density amplitude of the semiannual effect has increased by a factor of about 2 in Figure 8 while, for comparison, in the case of the geomagnetic activity effect the relative density amplitude of heat source II increased by a factor of 30 within the same height range (see Figure 2).

From Figure 9 we notice a time delay of 23 days between heat source I and its correspondent density variation. This is the observed time lag of the density maximum of the semiannual effect with respect to the equinoxes. It suggests that the heat source of the semiannual effect is in phase with the equinox.

The total energy amplitude of heat source I necessary to generate the observed relative density amplitude at 400 km altitude is

$$(\Delta E_0)_{semi} = 0.03 \text{ erg/cm}^2\text{sec} . \quad (8)$$

It gives rise to a temperature amplitude at 400 km height of

$$\Delta T_0 = 15^\circ\text{K} .$$

This temperature amplitude is smaller by a factor of 4 than Jacchia's exospheric temperature amplitude. The difference is quite understandable in the light of the density and temperature profiles in our model which are completely different from Jacchia's profiles (see Figure 8, where the dashed lines show the relative density and temperature amplitudes of the Jacchia model).

A semiannually varying energy input of heat source I with the constant amplitude of Equation (8) creates an absolute density amplitude at 400 km altitude which varies by a factor of 5 between solar minimum and solar maximum. This is shown in Figure 10 where absolute density and temperature amplitudes are plotted versus solar activity factor \bar{F} . This result is in excellent agreement with the observations as can be seen from the dashed line in Figure 10a. That curve has been calculated from Jacchia's formula of the semiannual variation of the exospheric temperature, converted into density amplitudes at 400 km altitude from his static diffusion model (Jacchia, 1964). We notice that such density increase with \bar{F} results exclusively from the change in the propagation conditions for the neutral waves within the thermosphere considering the fact that the amplitude of the heat source has been kept constant during the solar cycle.

Contrary to the behavior of the density amplitude the temperature amplitude in Figure 10b shows a slight decrease with increasing \bar{F} . Moreover its value is far below Jacchia's exospheric temperature amplitude that describes the semi-annual effect (the dashed line in Figure 10b).

The amplitude of heat source I of $0.03 \text{ erg/cm}^2\text{sec}$ [see Equation (8)], necessary to generate the observed semiannual density variations, is a reasonably small fraction of the mean total tidal wave energy of $(\bar{E}_0)_{\text{semi}} \sim 0.1 \text{ erg/cm}^2\text{sec}$ which is dissipated within the thermosphere (see paper I). Therefore, we conclude that the residual energy of the diurnal component of the tidal wave at 100 km height generated within the lower atmosphere varies by a factor of about 2 between solstitudes and equinox.

Heat source I which is the most likely energy distribution to generate the semiannual variation can of course only approximate the real situation. The tidal wave, whose energy is supposed to be dissipated within the thermosphere, penetrates high into the thermosphere (see paper I, Figure 5). However, the height distribution of the dissipated wave energy follows an exponential law with a scale height much smaller than that of heat source II (which is $H = 100 \text{ km}$). Moreover, as we can see from a comparison between the energies ΔE_0 of the three heat sources (see the tables in Figures 2, 5, 8), the energy input into the lower thermosphere, represented by heat source I, becomes with increasing period increasingly more important for the generation of density variations within the upper part of the thermosphere.

For these two reasons and from the results in this section we can conclude that the dissipation of the tidal wave energy and its semiannual

variation predominantly occurs within the lower thermosphere below 120 km altitude and that the energy dissipation above that height range has only a small effect upon the density variations within the entire thermosphere.

7. CONCLUSION AND DISCUSSION

Three kinds of density disturbances within the thermosphere which are nearly independent of local time — the geomagnetic activity effect, 27 day variations and semiannual variation — have been treated theoretically using a one dimensional model of the thermosphere in order to find out their generation mechanism and the amount of energy necessary to generate the observed density variations between 120 and 400 km altitude.

Three types of heat energy sources have been chosen in the calculations which simulate an energy input (see Figure 1):

- I from the bottom of the thermosphere
- II within the entire thermosphere
- III from the top of the thermosphere

The geomagnetic activity effect and the 27 day variations can be explained as generated by energy inputs of the general form of heat source II. The origin of the geomagnetic activity effect is interpreted as resulting from corpuscular radiation into the aurora zones and from a subsequent heat distribution by heat conduction and heat convection into the lower latitudes which is in agreement with earlier ideas (Jacchia, 1966). The time delay of the density variation with respect to the heat input is about 6 hours and is nearly independent of height above 200 km also in agreement with the observations (Jacchia et al., 1966;

Roemer, 1967a). The theoretical results exclude a heat input from below (heat source I) or from the exosphere (heat source III) as a possible cause of the geomagnetic activity effect.

The theoretical calculations of the 27 day variation support the idea that it is generated by excessive solar EUV radiation from activity centers on the sun. Here the time lag between maximum heating and maximum density is 2 days in sufficient agreement with the observations (MacDonald, 1963, Roemer, 1967b).

The semiannual effect can be described by heat source I (heat input below 120 km altitude) which shows the observed large density variation below 200 km and the slow increase of the relative density amplitude with height. Moreover the observed dependence of the density amplitudes on the solar activity factor \bar{F} can be correctly reproduced. The time lag between maximum heating and maximum density is about 20 days. The semiannual effect is interpreted as resulting from the semiannual variation of the tidal wave from the lower atmosphere which is dissipated within the thermosphere. This variation follows from the semi-annually varying leakage of energy of the diurnal component of the tidal wave from the lower into the upper atmosphere which is due to semiannual variations in the global stratospheric and mesospheric winds systems. From the theoretical results a heat input from the exosphere or within the thermosphere (heat sources II and III) can be excluded as the origin of the semiannual effect.

While the observed density disturbances can be reasonably well reproduced in our model, the calculated temperature variations do not agree so well with the temperature amplitudes derived from the Jacchia model. This is especially true during the semiannual effect where our temperature amplitude is smaller

by a factor varying from 2 to 8 with solar activity as compared with Jacchia's data. The main reason for this discrepancy is the difference between the density-height profiles in both models which becomes especially large during the semiannual effect. However, in our model we neglected the temporal variations of the composition of the neutral air. As shown in part I of this paper this gives rise to a value in the calculated temperature amplitude too low by about 30% at 400 km altitude. In the case of the semiannual effect the correction of such error would diminish the ratio between Jacchia's and our temperature amplitude to the factor 1.5 to 6. Even then is our temperature amplitude significantly smaller than Jacchia's value which results from the two different temperature-height profiles adopted in both models.

The altitude of 400 km is the upper limit of our model. Below that height composition changes are only of small influence for the dynamics of the thermosphere. Above that height range the composition changes predominate the total density and temperature variations. However, these problems are outside the scope of this paper.

ACKNOWLEDGEMENT

I am very indebted to H. G. Mayr and G. P. Newton for most exciting and stimulating discussions.

LITERATURE

Becker, W., 1966, in Frihagen (ed) "Electron density profiles in ionosphere and exosphere", North-Holland Publ. Com., Amsterdam, pp. 218-230.

Blum, P. W., 1969, Planet. Space Sci. (to be published)

Cole, K. D., 1966, Space Sci. Rev. 5, 700-770

Cook, G. E., 1966, Royal Aircraft Establ., Tech. Rep. RAE-TR-66211, Farnborough.

Cook, G. E. and D. W. Scott, 1966, Planet. Space Sci. 14, 1149-1165

Dessler, A. J., 1958, Journ. Geophys. Res. 63, 405-408

Harris, I. and W. Priester, 1969, submitted to Journ. Atm. Sci.

Jacchia, L. G., 1959, Nature 183, 526-527

Jacchia, L. G., 1964, Special Report 170, Smithsonian Institution, Astrophysical Observatory, Cambridge, Mass.

Jacchia, L. G., 1965, Space Research V, North-Holland Publ. Comp., Amsterdam, p. 1152

Jacchia, L. G., 1966, Ann. Geophys. 22, 75-85

Jacchia, L. G. and R. E. Briggs, 1958, Special Report 18, Smithsonian Institution, Astrophysical Observatory, Cambridge, Mass.

- Jacchia, L. G. and J. W. Slowey, 1964a, Space Research IV, North-Holland Publ. Comp., Amsterdam, pp. 257-270
- Jacchia, L. G. and J. W. Slowey, 1964b, Journ. Geophys. Res. 69, 905-910
- Jacchia, L. G., J. W. Slowey, and I. G. Campbell, 1968, Special Report 265, Smithsonian Institution, Astrophysical Observatory, Cambridge, Mass.
- Jacchia, L. G., J. W. Slowey, and F. Verniani, 1966, Special Report 218, Smithsonian Institution, Astrophysical Observatory, Cambridge, Mass.
- King-Hele, D. C., 1967, Nature 216, 880
- Kochanski, A., 1964, Journ. Geophys. Res. 69, 3651-3662
- Langel, R. A. and J. C. Cain, 1968, Ann. Geophys. 24, 857-869
- Lauter, E. A., J. Hruskova, G. Nestrorov, and K. Sprenger, 1966, in E. A. Lauter (ed) "Vorträge Sommerschule Kühlungsborn, Vol II/1, Berlin
- MacDonald, G. F. C., 1963, Rev. Geophys. 1, 305-349
- Newell, R. E., 1968, Nature 217, 150
- O'Brien, B. J. and H. Taylor, 1964, Journ. Geophys. Res., 64, 45-63
- Pätzold, H. K. and H. Zschörner, 1960, Space Research I, North-Holland Publ. Comp., Amsterdam, pp. 24-36
- Priester, W., 1959, Naturwissenschaften, 46, 197-198
- Priester, W. and D. Cattani, 1962, Journ. Atm. Sci. 19, 121-126

Priester, W., M. Roemer, and H. Volland, 1967, Space Sci. Rev. 6, 707-780

Quiroz, R. S. and A. J. Miller, 1967, Monthly Weather Rev. 95, 635-641

Roemer, M., 1967a, Phil. Trans. Roy. Soc., A 262, 185-194

Roemer, M., 1967b, Space Research VII, North-Holland Publ. Comp., Amsterdam,
pp. 1091-1099

Thomas, G. E. and B. K. Ching, 1968, Aerospace Corporation, Air Force Report
No. SAMSO-TR-68-57, Los Angeles

Volland, H., 1967, Journ. Geophys. Res. 72, 2831-2841

Volland, H., 1968, NASA document X-621-68-503, Goddard Space Flight Center,
Greenbelt, Md.

Wagner, C. U., 1968, Journ. Atm. Terr. Phys. 30, 579-589

Yonezawa, T., 1967, Journ. Radio Res. Lab., Tokyo, 14, 1-25

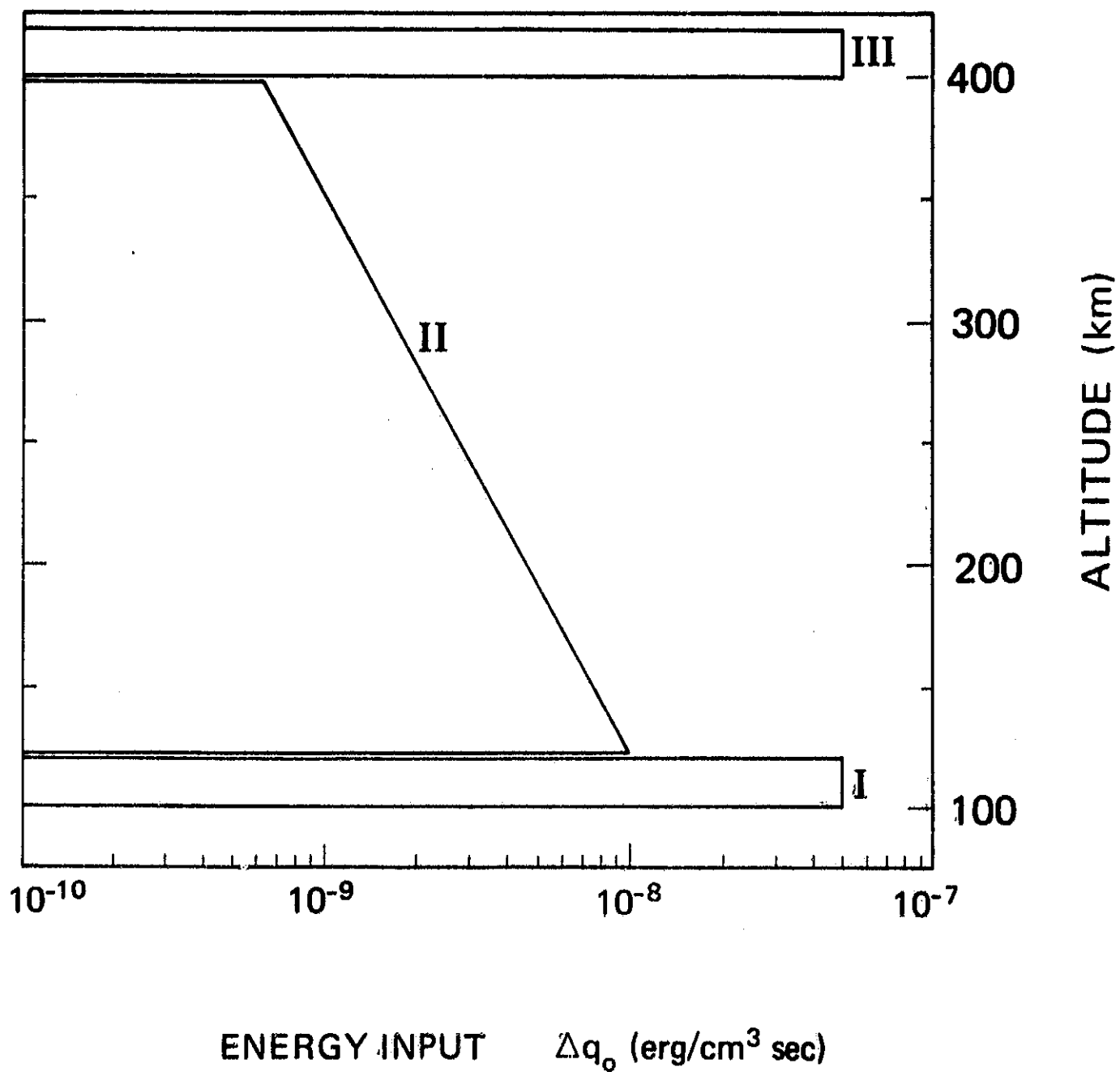


Figure 1. Energy distribution versus height of the amplitude Δq_0 of three different heat sources harmonically varying in time which simulate energy input at the bottom (I) within the entire thermosphere (II), and at the top (III) of the thermosphere. The integral energy amplitude of each heat source is $\Delta E_0 = 0.1 \text{ erg/cm}^2 \text{ sec}$.

GEOMAGNETIC ACTIVITY EFFECT RELATIVE AMPLITUDE OF

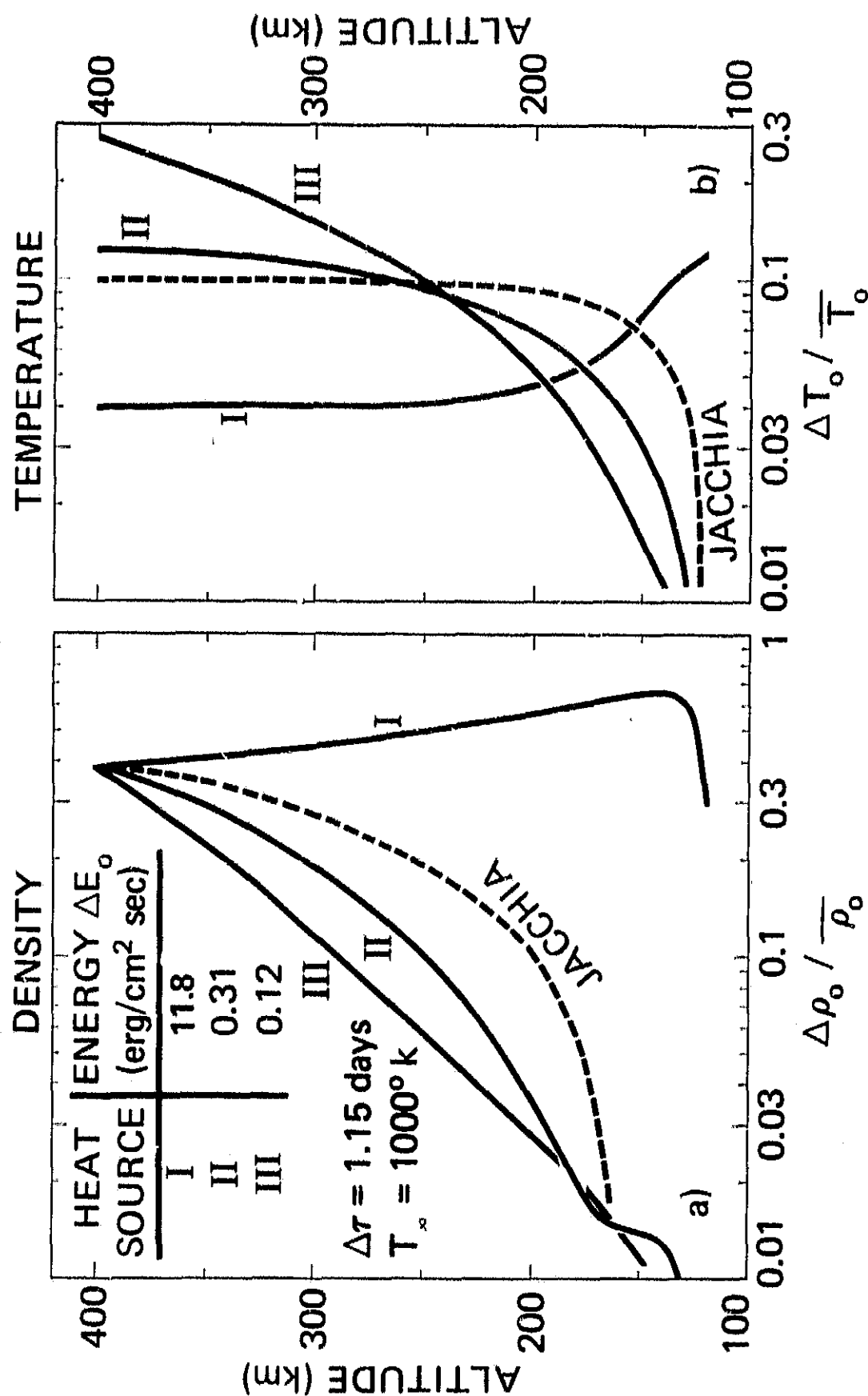


Figure 2. Relative density amplitude (Figure 2a) and relative temperature amplitude (Figure 2b) versus height generated by three different heat sources which represent energy input at the bottom (I) into the entire thermosphere (II), and at the top (III) of the thermosphere during a geomagnetic activity effect. The dashed lines are derived from the Jacchia model (Jacchia, 1964) for $T_\infty = 1000^\circ \text{K}$ and $\Delta T_\infty = 100^\circ \text{K}$.

GEOMAGNETIC ACTIVITY EFFECT TIME LAG OF

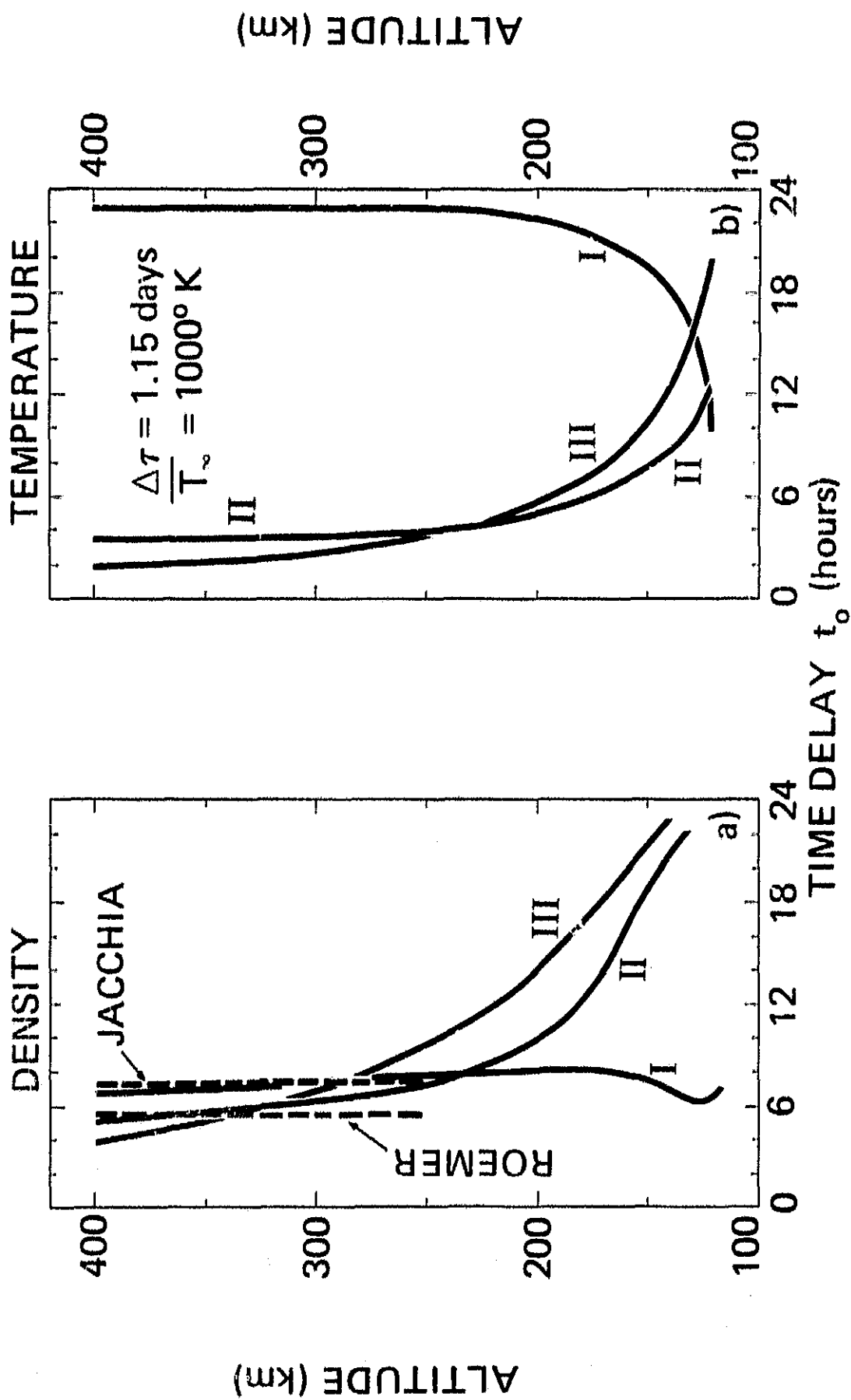


Figure 3. Time lag versus height of density maximum (Figure 3a) and temperature maximum (Figure 3b) with respect to the maximum heat input of heat sources I, II and III during a geomagnetic activity effect. The dashed lines in Figure 3a give data observed by Roemer (1967a) and Jacchia et al. (1966).

GEOMAGNETIC ACTIVITY EFFECT

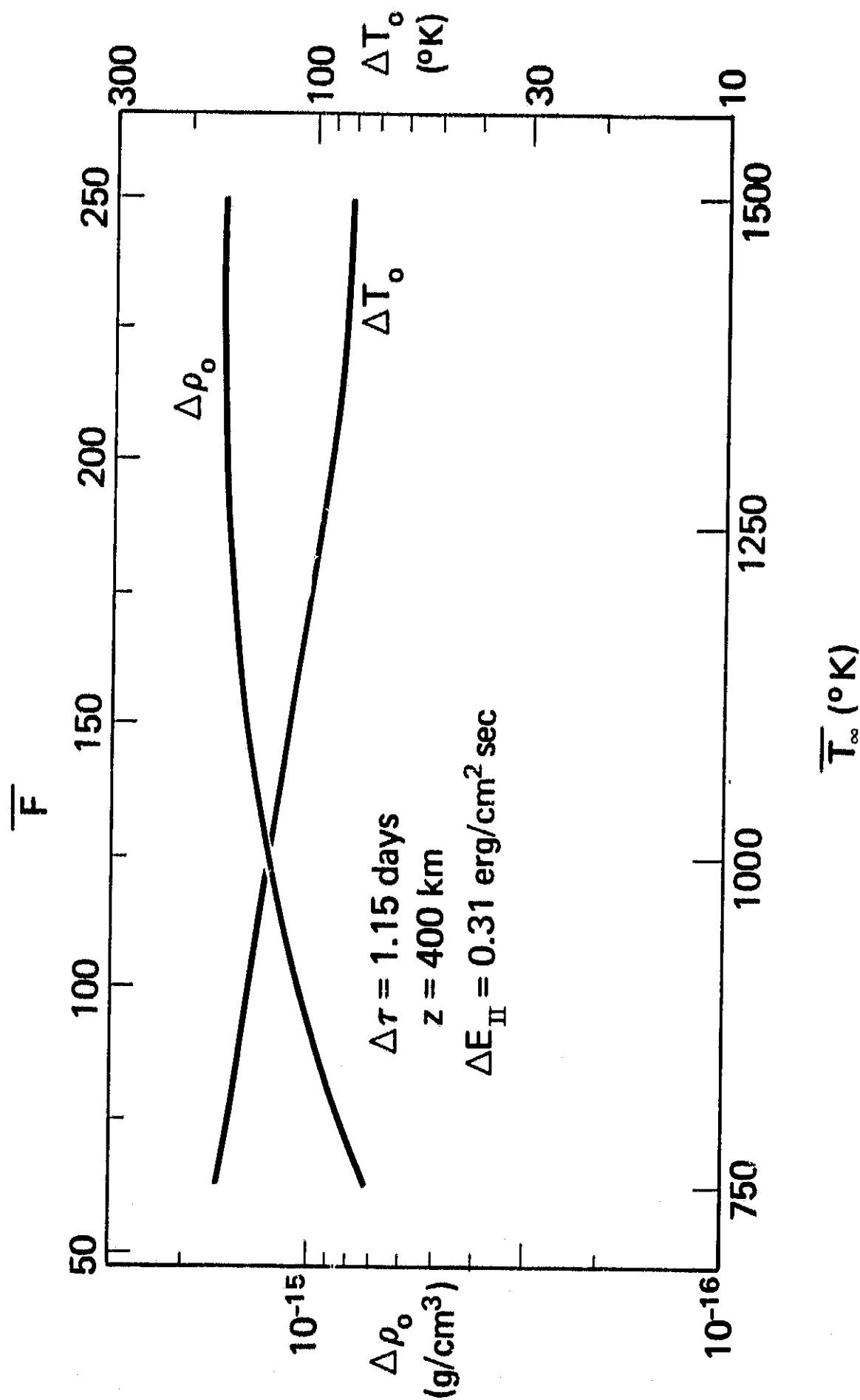


Figure 4. Absolute amplitudes at 400 km altitude of density and temperature versus solar activity factor \bar{F} which are generated by heat source II of constant energy amplitude $\Delta E_{II} = 0.31 \text{ erg/cm}^2 \text{ sec}$ during a geomagnetic activity effect.

27 DAY SOLAR ROTATION RELATIVE AMPLITUDE OF

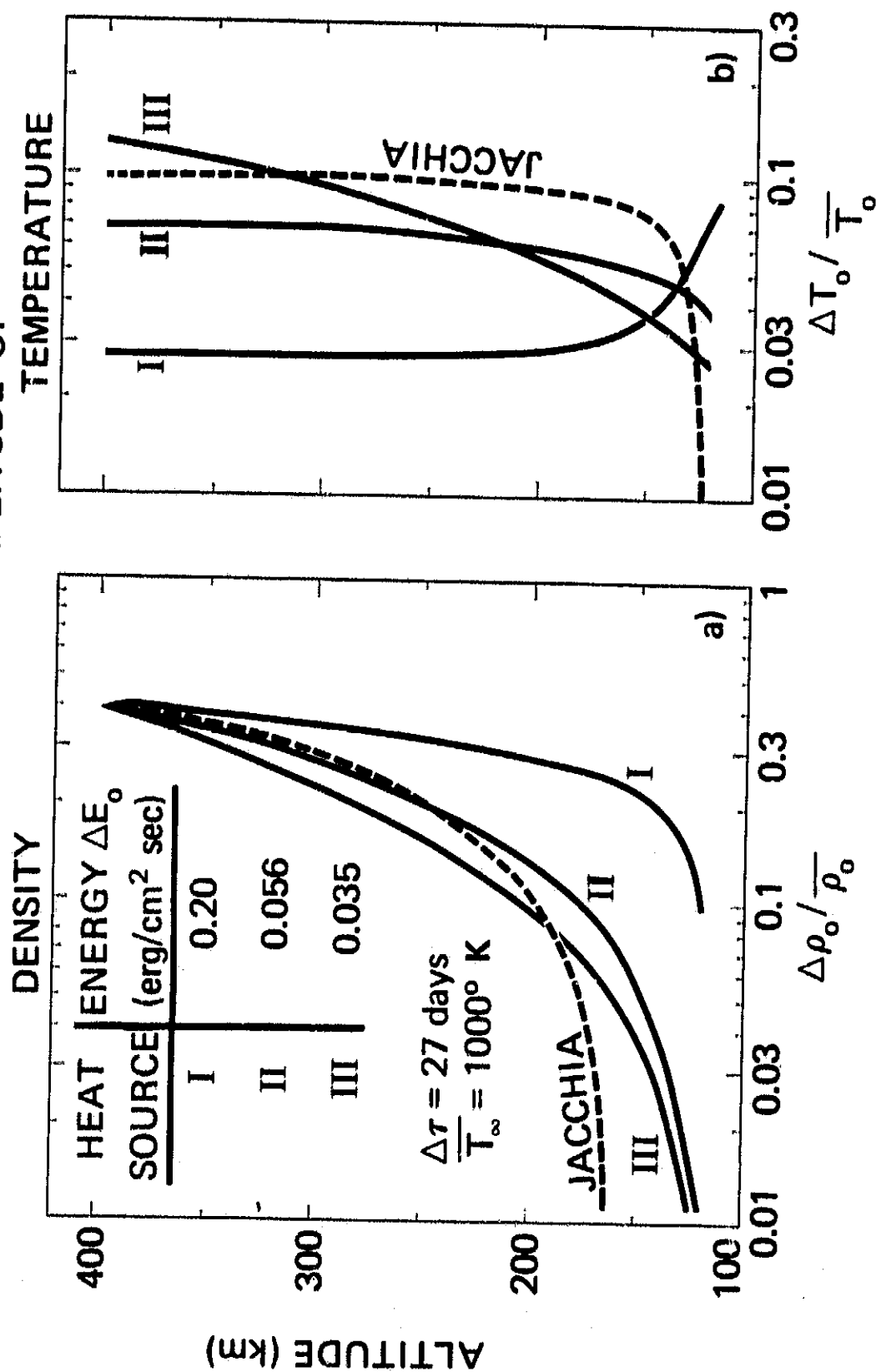


Figure 5. Relative density amplitude (Figure 5a) and relative temperature amplitude (Figure 5b) versus height generated by three different heat sources which represent energy input at the bottom (I) into the entire thermosphere (II), and at the top (III) of the thermosphere during the 27 day variation. The dashed lines are derived from the Jacchia model (Jacchia, 1964) for $T_\infty = 1000^\circ \text{K}$ and $\Delta T_\infty = 100^\circ \text{K}$.

27 DAY SOLAR ROTATION

TIME LAG OF

DENSITY

TEMPERATURE

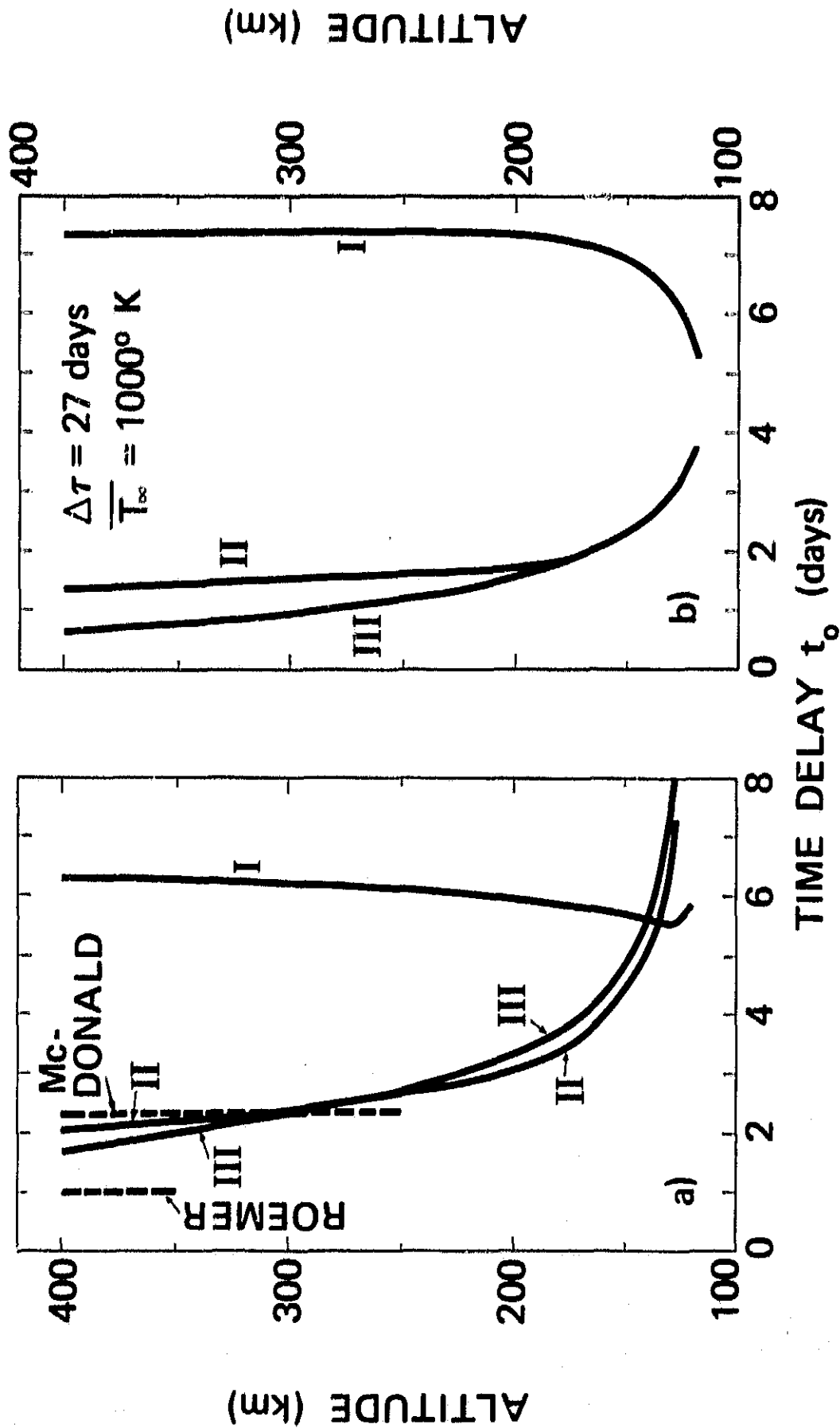


Figure 6. Time lag versus height of density maximum (Figure 6a) and temperature maximum (Figure 6b) with respect to the maximum heat input of heat sources I, II and III during the 27 day variation. The dashed lines in Figure 6a give data observed by Roemer (1967b) and MacDonald (1963).

27 DAY SOLAR ROTATION

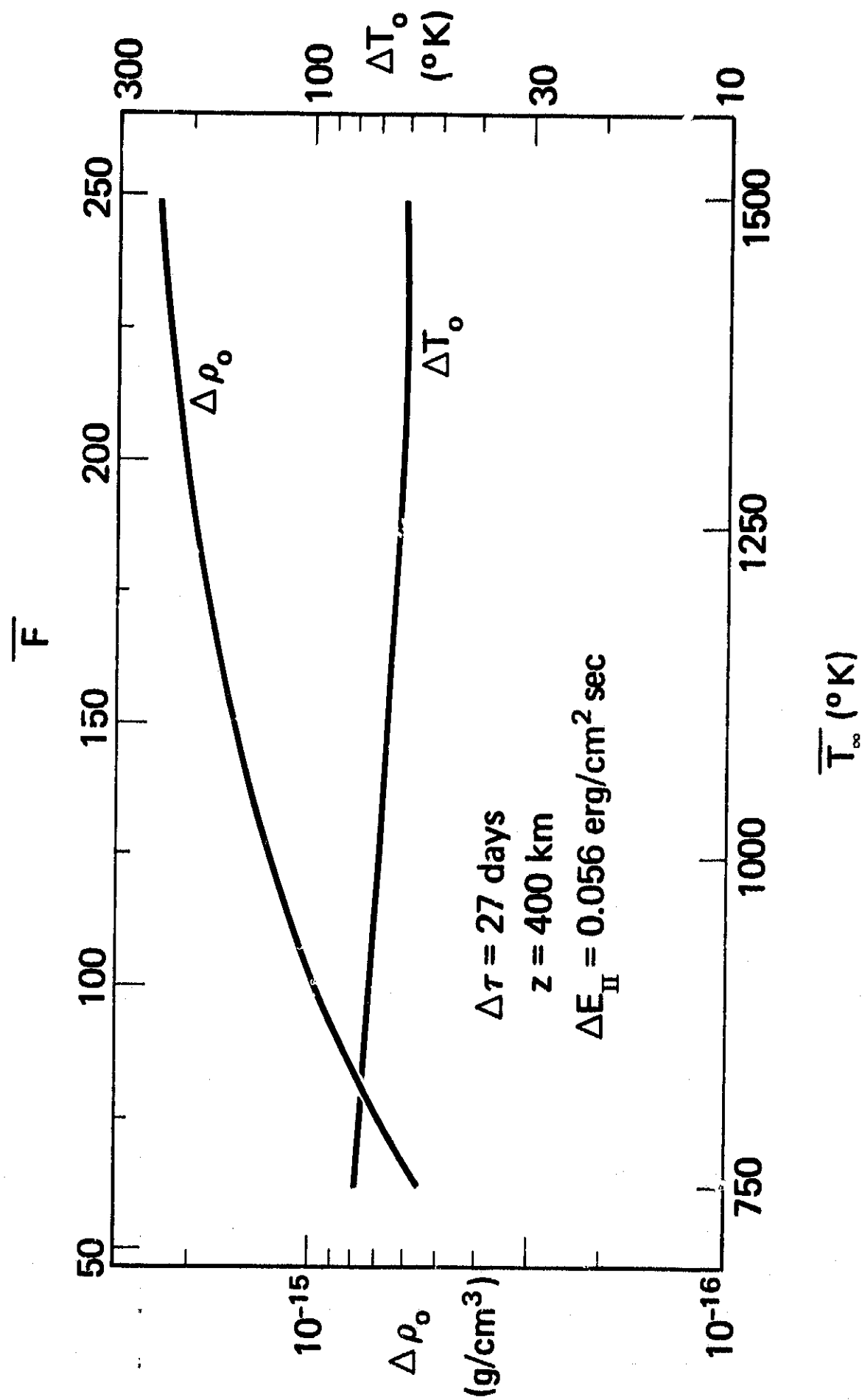


Figure 7. Absolute amplitudes of density and temperature at 400 km altitude versus solar activity factor \bar{F} which are generated by heat source II of constant energy amplitude $\Delta E_{\text{II}} = 0.056 \text{ erg/cm}^2 \text{ sec}$ during the 27 day variation.

SEMIANNUAL EFFECT RELATIVE AMPLITUDE OF

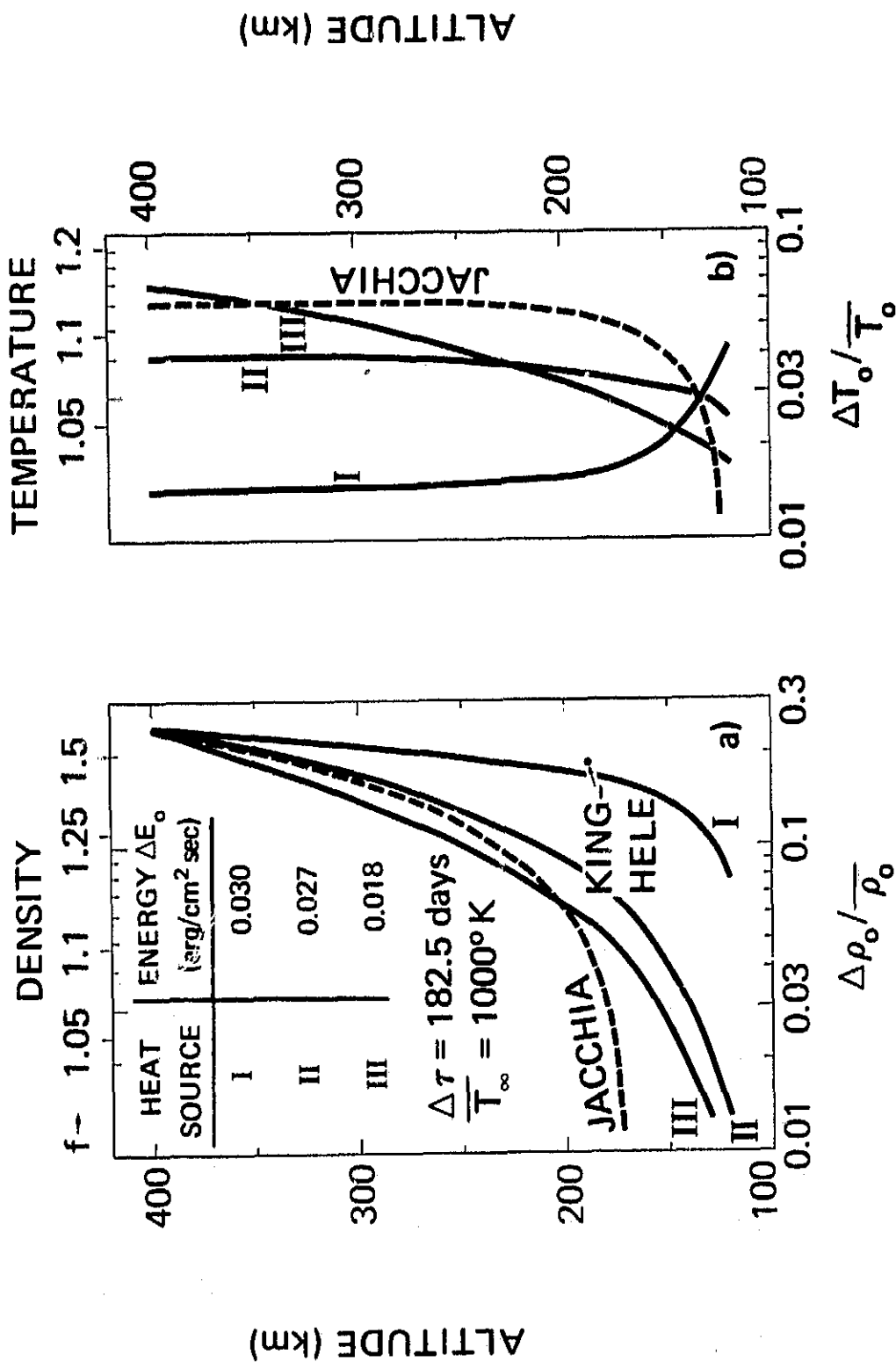


Figure 8. Relative density amplitude (Figure 8a) and relative temperature amplitude (Figure 8b) versus height generated by three different heat sources which represent energy input at the bottom (I) into the entire thermosphere (II), and at the top of the thermosphere (III) during the semiannual variation. The dashed lines are derived from the Jacchia model (Jacchia, 1964) for $T_\infty = 1000^\circ \text{K}$ and $\Delta T_\infty = 60^\circ \text{K}$. The full circle in Figure 8a gives a measured value (King-Hele, 1967). Upper scales give the ratio between maximum and minimum value $f = c_{\text{max}}/c_{\text{min}}$.

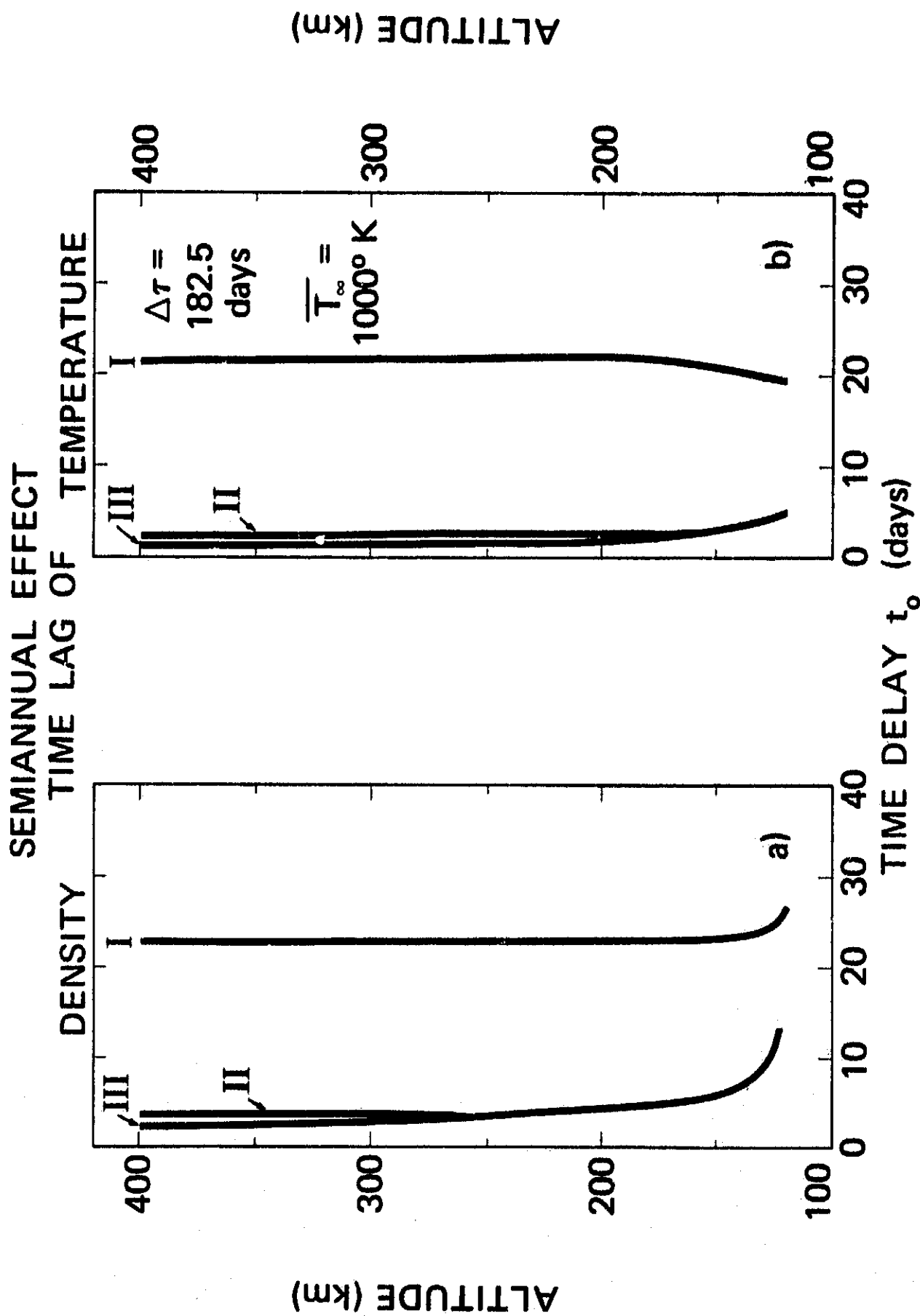


Figure 9. Time lag versus height of density maximum (Figure 9a) and temperature maximum (Figure 9b) with respect to the maximum heat input of heat sources I, II and III during the semiannual variation.

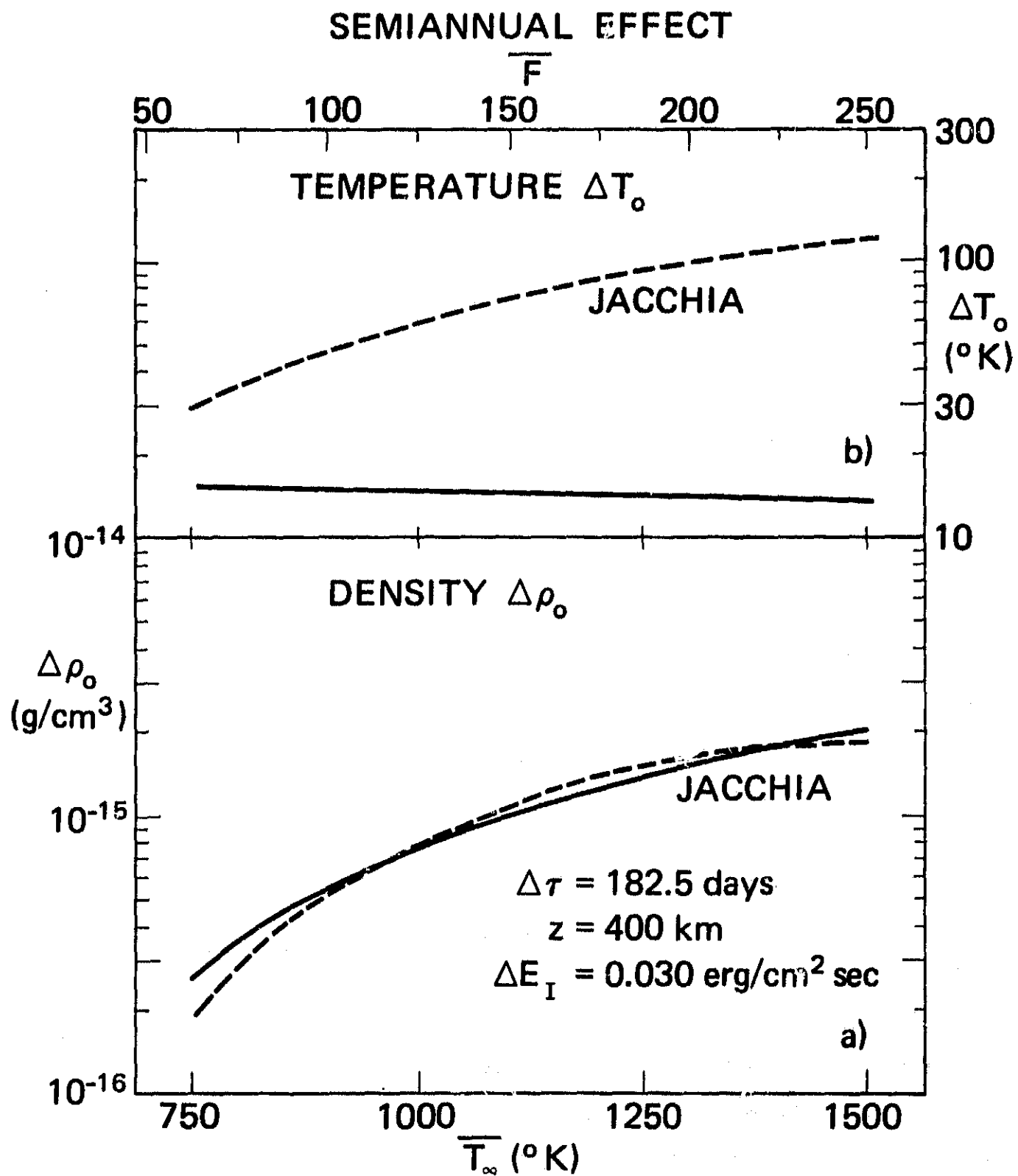


Figure 10. Absolute amplitudes of density (Figure 10a) and of temperature (Figure 10b) at 400 km altitude versus solar activity factor \overline{F} which are generated by heat source I of constant energy amplitude $\Delta E_I = 0.030$ erg/cm²sec during the semiannual variation. The dashed lines are derived from Jacchia's formula of the semiannual variation of his exospheric temperature and from his static diffusion model (Jacchia, 1964).